Biophysical Journal
Article

Biophysical Society

Propagation Failure by TRPM4 Overexpression

Namit Gaur,[1,2] Thomas Hof,[2,3] Michel Haissaguerre,[2,4] and Edward J. Vigmond[1,2,*]
[1]University Bordeaux, IMB UMR 5251, Talence, France; [2]IHU Liryc, Electrophysiology and Heart Modeling Institute, Fondation Bordeaux Université, Pessac-Bordeaux, France; [3]Université Bordeaux, Centre de recherche Cardio-Thoracique de Bordeaux, U1045, Bordeaux, France; and [4]Bordeaux University Hospital (CHU), Cardiac Electrophysiology and Cardiac Stimulation Team, Pessac, France

ABSTRACT Transient receptor potential melastatin member 4 (TRPM4) channels are nonselective monovalent cationic channels found in human atria and conduction system. Overexpression of TRPM4 channels has been found in families suffering from inherited cardiac arrhythmias, notably heart block. In this study, we integrate a mathematical formulation of the TRPM4 channel into a Purkinje cell model (Pan-Rudy model). Instead of simply adding the channel to the model, a combination of existing currents equivalent to the TRPM4 current was constructed, based on TRPM4 current dynamics. The equivalent current was then replaced by the TRPM4 current to preserve the model action potential. Single-cell behavior showed early afterdepolarizations for increases in TRPM4 channel expression above twofold. In a homogeneous strand of tissue, propagation conducted faithfully for lower expression levels but failed completely for more than a doubling of TRPM4 channel expression. Only with a heterogeneous distribution of channel expression was intermittent heart block seen. This study suggests that in Purkinje fibers, TRPM4 channels may account for sodium background current (I_{Nab}), and that a heterogeneous expression of TRPM4 channels in the His/Purkinje system is required for type II heart block, as seen clinically.

INTRODUCTION

The transient receptor potential melastatin 4 (TRPM4) channel is a homotetrameric nonselective channel permeable to monovalent cations but not to Ca^{2+} (permeability sequence: $Na^+ \approx K^+ > Cs^+ > Li^+ \gg Ca^{2+}$) (1,2). It harbors a linear unitary current-voltage relationship and a conductance of 20–25 pS (1), and its open probability increases with depolarization and intracellular Ca ($[Ca]_i$) (3). At the whole-cell level, 10 μM $[Ca]_i$ is sufficient to elicit a typical TRPM4 outward rectifying current in a heterologous expression system, suggesting that physiological ranges of $[Ca]_i$ rises (subsarcolemmal [Ca] of 10–15 μM in cardiac cells (4)) are able to activate the channel. TRPM4 messenger RNA and protein are highly expressed in the heart, especially in the conductive tissue. It participates in the electrical activity of several cardiac structures, including Purkinje fibers (PF) (5).

TRPM4 gene mutation was first reported as the cause of the autosomal-dominant form of progressive familial heart block type I in a large Afrikaaner pedigree (6). Liu et al. (7) demonstrated three other TRPM4 mutations in familial cases of idiopathic cardiac conduction disease. Several other mutations have been found in families with autosomal-dominant inherited conduction blocks, including bundle branch blocks (8–11). Most mutations result in impaired SUMOylation and endocytosis of TRPM4 channels, resulting in overexpression of channel density and currents on the sarcolemma (6,7,11). Despite its role in regulating the conduction activity in PF and in causing inherited conduction blocks, the arrhythmogenic mechanisms behind such activity by TRPM4 channels remain elusive.

In this work, we develop a, to our knowledge, novel mathematical formulation of TRPM4 channel current using available experimental data on activation of TRPM4 channels by voltage and $[Ca]_i$. The channel current is integrated into a Purkinje cell ionic model (Pan-Rudy model (PRd)) (12). We investigate single-cell behavior and propagation in a PF with a heterogeneous channel distribution. Results indicate that overexpression of TRPM4 channels can lead to early afterdepolarizations (EADs) in single cells. Only with a heterogenous distribution of TRPM4 channels in PF, complex patterns of conduction blocks, such as type I, II, and III, pacemaking activity, and repolarization failure, are observed. This study demonstrates mechanisms behind complex patterns of conduction block due to overexpression of TRPM4 channels. It also shows that background ionic currents in cell models may represent as yet uncharacterized currents.

Submitted September 24, 2018, and accepted for publication November 27, 2018.

*Correspondence: edward.vigmond@u-bordeaux.fr

Editor: Michael Pusch.
https://doi.org/10.1016/j.bpj.2018.11.3137

MATERIALS AND METHODS

Channel formulation

TRPM4 gene encodes a nonselective cation channel that is roughly equally permeable to Na^+ and K^+ (13). TRPM4 current is sensitive to $[Ca]_i$, which activates the channel, and to voltage, which evokes higher activity in the positive voltage range (1,14). Inside-out patch-clamp experiments of single channel activity revealed that the reversal potential of TRPM4 channel is close to zero (0.2 mV), indicating that the channel does not differentiate among monovalent cations (13). Mean open channel probability (P_o) is an increasing function of membrane voltage, and the channel activity is higher at depolarized potentials. These data are fit to a Boltzmann function to develop a voltage activation gate of the channel. The EC_{50} of $[Ca]_i$ activation is 1.3 μM, close to peak systolic $[Ca]_i$ values (15). Accordingly, we used these data to fit the calcium-activation gate for the channel. The channel opening is assumed to respond instantaneously to voltage and with a slower dynamic to $[Ca]_i$ changes. Assembled together, the formulation for TRPM4 channel current can be written as

$$I_{\mathrm{TRPM4}} = \overline{g}_{\mathrm{TRPM4}} \times X_{\mathrm{Cai}} \times X_{\mathrm{V}} \times (V - E_{\mathrm{TRPM4}}), \quad (1)$$

$$= I_{\mathrm{Na,TRPM4}} + I_{\mathrm{K,TRPM4}}, \quad (2)$$

$$\frac{dX_{\mathrm{Cai}}}{dt} = \frac{X_{\mathrm{Cai}}^{\infty} - X_{\mathrm{Cai}}}{\tau_{X_{\mathrm{Cai}}}}, \quad (3)$$

$$X_v = 0.05 + \frac{0.95}{1 + e^{-(V-40)/15}}, \quad (4)$$

$$X_{\mathrm{Cai}}^{\infty} = \frac{1}{1 + \left(\lceil Ca^{2+} \rceil_{\mathrm{SSL}}/0.0013\right)^{-1.1}}, \quad (5)$$

$$\tau_{X_{\mathrm{Cai}}} = 30, \quad (6)$$

$$I_{\mathrm{Na,TRPM4}} = g_{\mathrm{Na,TRPM4}} \times (V - E_{\mathrm{Na}}), \quad (7)$$

and

$$I_{\mathrm{K,TRPM4}} = g_{\mathrm{K,TRPM4}} \times (V - E_{\mathrm{K}}). \quad (8)$$

V is the transmembrane voltage (mV), and E_X is the reversal potential for species X. $\overline{g}$ is the maximal conductance of the channel (mS/cm^2), and $\tau_{X_{\mathrm{Cai}}}$ is the time constant for Ca-dependent changes (ms). X_v is the voltage activation gate, and X_{Cai} is the calcium-activation gate. To decompose I_{TRPM4} into its constituent currents $I_{\mathrm{Na,TRPM4}}$ and $I_{\mathrm{K,\ TRPM4}}$, we used the fact that at $V = E_{\mathrm{TRPM4}}$ and $I_{\mathrm{TRPM4}} = 0$ to solve the conductance values for Na^+ and K^+ currents through TRPM4 channels:

$$g_{\mathrm{K,TRPM4}} = I_{\mathrm{TRPM4}} \times \frac{E_{\mathrm{TRPM4}} - E_{\mathrm{Na}}}{(V - E_{\mathrm{Na}})(E_{\mathrm{K}} - E_{\mathrm{TRPM4}}) + (V - E_{\mathrm{K}})(E_{\mathrm{TRPM4}} - E_{\mathrm{Na}})} \quad (9)$$

$$g_{\mathrm{Na,TRPM4}} = I_{\mathrm{TRPM4}} \times \frac{E_{\mathrm{K}} - E_{\mathrm{TRPM4}}}{(V - E_{\mathrm{Na}})(E_{\mathrm{K}} - E_{\mathrm{TRPM4}}) + (V - E_{\mathrm{K}})(E_{\mathrm{TRPM4}} - E_{\mathrm{Na}})} \quad (10)$$

The PRd of the canine Purkinje cell (12) was chosen for the study because it is the only model that captures the three-tier Ca-release process, and TRPM4 channel opening is primarily dependent on $[Ca]_i$. The model prediction matches experimental data as shown in Fig. 1 *A*. The species ionic currents ($I_{\mathrm{Na,\ TRPM4}}$, $I_{\mathrm{K,\ TRPM4}}$) are used to determine the balance of Na^+ and K^+ flowing through TRPM4 channels. Na^+ flows into the subsarcolemma (SSL), and K^+ flows out of the bulk myoplasm of the Purkinje cell. Both cell and cable simulations were run till dynamic steady state was reached, and changes in state variables from beat to beat were <0.01%.

Cable behavior classification

The following are the definitions of cable behavior in Table 1. The 1:1 refers to normal conduction along the cable. First-degree block occurs when the impulse reaches the right end after a delay of more than 40 ms. The cable is quiescent when it cannot be excited. Second-degree block occurs when some of the impulses fail to propagate to the right end. When no impulse reaches the right end, the cable has a third-degree block. If there are spontaneous action potentials (APs) in the cable, then the cable has a pacemaker behavior. If some APs in the left or right end nodes fail to repolarize before the impulse reaches the node, then the cable has repolarization failure. The criteria is applied sequentially from top to bottom of the table so that there can only be one type of cable behavior. Thus, e.g., the cable cannot have both repolarization failure and a second-degree block.

Software

The Cardiac Arrhythmia Research Package was used for single-cell and cable simulations (16). The bench module was used for single-cell simulations. MagicPlot Student v2.7.2 and Grace v5.1.25 were used as plotting software. MATLAB R2015b (The MathWorks, Natick, MA) was used for data analysis.

RESULTS

Incorporation into an existing Purkinje cell model

Published cell models are tuned to recreate measured experimental behavior. Of particular note is that TRPM4-channel block leads to a dramatic AP duration (APD) shortening (13). Hu et al. (17) has been the only group to add a TRPM4 channel current to several ionic models, but no attempt was made to adjust for control APs. Simply adding a current of such magnitude to existing models greatly affects the APs, such that AP no longer corresponds to the measured AP-fitting data (see Fig. 2). Thus, it was reasoned that the effect of TRPM4 current had to have been implicitly incorporated but was distributed among the channels represented in models.

The first step was to compute the expected TRPM4 channel current, I_{TRPM4}. This was calculated by applying the nominal model AP shape and $[Ca]_i$ time trace (i.e., $[Ca^{2+}]_{\mathrm{SSL}}$) to the channel formulation at pacing cycle length (PCL) = 1000 ms. Next, by analyzing kinetic profiles of the existing monovalent ion currents, a combination of these currents equivalent to I_{TRPM4} was determined (see Fig. 3 for the major monovalent ionic currents). The TRPM4 current had a constant component during the resting phase, which could only be matched by the background sodium current (I_{Nab}) because all other inward currents were near zero. We assumed that all of I_{Nab} was composed of I_{TRPM4}, and this allowed us to

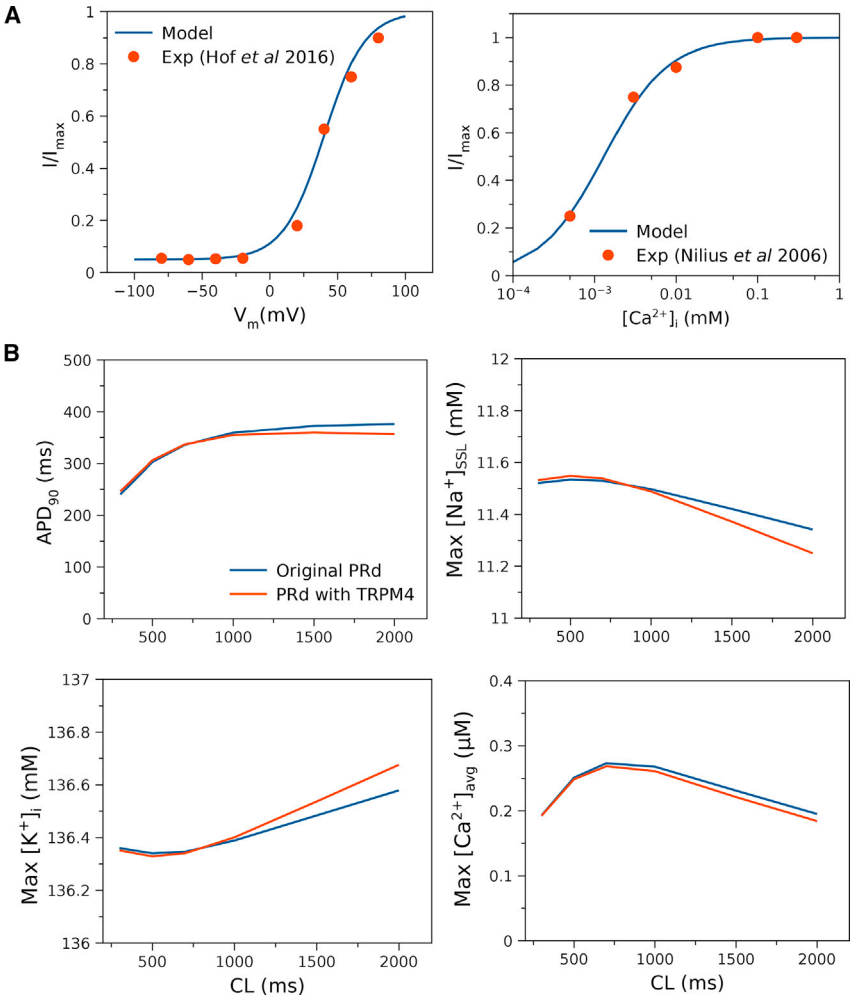

FIGURE 1 Validation of the TRPM4 channel current formulation in the Purkinje cell model (PRd). (*A*) Model fit to experimental data on voltage-dependent activation (13) and Ca-dependent activation of the channel (15). The currents are normalized to correspond to normalized open probability P_o data. (*B*) Rate dependence of original PRd (12) and PRd with TRPM4 channel current formulation for action potential duration (APD), maximal $[Na^+]$ in the subsarcolemma ($[Na^+]_{SSL}$), maximal $[K^+]$ in the bulk myoplasm ($[K^+]_i$), and maximal averaged $[Ca^{2+}]$ ($[Ca^{2+}]_{avg}$) agree with the original model values. Small differences occur at slow rates. $[Ca^{2+}]_{avg}$ is the spatially averaged $[Ca^{2+}]$ in peripheral coupling space, subsarcolemma (SSL), and bulk myoplasm (12). To see this figure in color, go online.

calibrate the conductance of I_{TRPM4}. The fitting was also constrained by considering that I_{TRPM4} could not be larger than the current component being replaced. Examining I_{TRPM4}, an initial large outward current was present that had to be K^+ current, and the only possible current with that profile was transient outward K^+ current type 1 (I_{to1}). In terms of magnitude, it was 10% of the initial I_{to1}. After adding this component to the equivalent current, the only candidate for matching the negative current during the AP plateau shape was the late sodium type 2 current, I_{NaL2}.

To capture the magnitude during the plateau, 33% of this current was added to the equivalent current. In summary, the best fit for the equivalent current, I_{Eqv}, was

$$I_{Eqv} = 0.1 \times I_{to1} + I_{Nab} + 0.33 \times I_{NaL2} \approx I_{TRPM4}, \quad (11)$$

expressed in terms of the originally published currents (see Fig. 3, *bottom*). There was a small difference in currents during repolarization that could not be removed without reformulating kinetics of some current, so it was left out. For our formulation, I_{Eqv} was removed from the original model by lowering the conductances of the selected channels, and the TRPM4 channel current was added. This was verified by comparing the AP shape between models. The voltage trace was relatively preserved with an APD increase of 20.3 ms and a slowing in peak repolarization rate from −660 to −534 mV/ms. Simulating block by 9-phenanthrol reduced APD by 29.1%, similar to that seen in rabbit Purkinje cells.

TABLE 1 Criteria for Classifying Cable Behavior

Behavior	Criteria
1:1	$A^L = A^R = N^P \wedge \forall i : \Delta t_i^R \leq 40$ ms
First-degree block	$A^L = A^R = N^P$
Quiescent	$A^L = A^M = A^R = 0$
Pacemaker	$\exists x : A^x > N^p \vee \exists i : \Delta t_i^L > 2$ ms
Second-degree block	$A^L > A^R > 0$
Third-degree block	$A^L > A^R = 0$
Repolarization failure	$A^L < N^p \wedge A^R > 0$
Other	–

Let A^X be the number of APs detected at node x, being the left (L), right (R), or middle (M) of the cable. N^P is the number of pulses delivered, and $\Delta t^X{}_i$ is the delay between AP i at node x and the last pacing beat. Tests proceeded in order from top to bottom and stopped when the set of criteria were met.

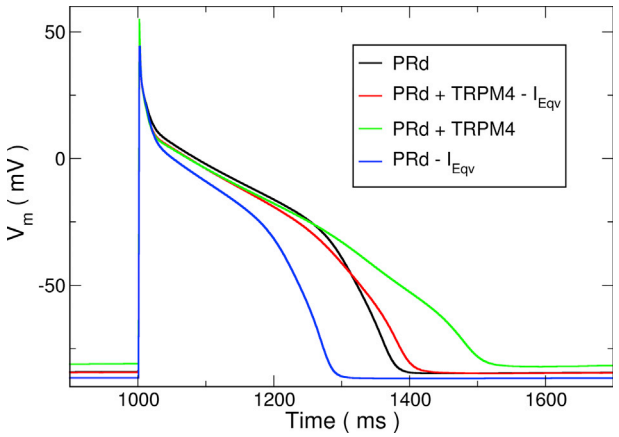

FIGURE 2 Effect of currents on simulated action potentials (APs) of PRd. The original AP as published (*black*) is shown. Addition of the TRPM4 current without any further modifications (*green*) resulted in a substantial APD prolongation. Additionally, removing the equivalent current I_{Eqv} (*red*) produced an AP much closer to the original. Simulated block of the TRPM4 channel with 9-phenanthrol (*blue*), which is equivalent to only subtracting I_{Eqv} from the original model, resulted in a 29.1% reduction in APD. To see this figure in color, go online.

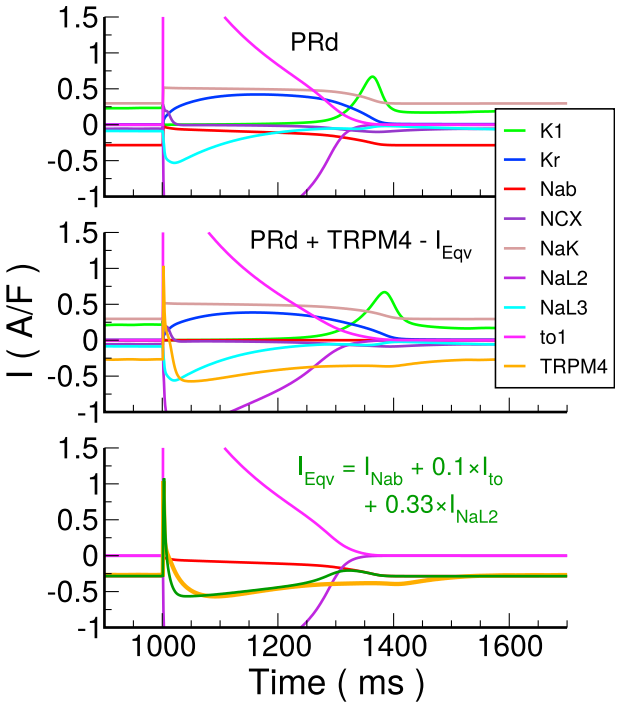

FIGURE 3 Major monovalent ionic currents for the Purkinje cell ionic model. Top: Original PRd model is shown. Middle: Adjusted model with TRPM4 channel current and I_{eqv} subtracted is shown. Bottom: I_{TRPM4} is compared to I_{Eqv} and its constituent currents. The cell was stimulated at pacing cycle length (PCL) = 1000 ms. Kr, rapidly activating delayed rectifier K^+ current; NCX, Na^+-Ca^{2+} exchanger current; NaK, Na^+-K^+ pump current; NaL2, NaL3, late Na^+ currents; to1, transient outward current type 1 carried by K^+. To see this figure in color, go online.

Rate dependence of APD and ionic concentrations in the cell (shown as maximal values of Na concentration in SSL ($[Na^+]_{SSL}$)), K concentration in the bulk myoplasm ($[K^+]_i$), and spatially averaged [Ca]$_i$ ($[Ca^{2+}]_{avg}$) is similar to the original PRd without TRPM4 channels (Fig. 1 *B*). Small differences occur at slow rates (PCL $>$ 1500 ms) and may be attributed to kinetic difference of TRPM4 current compared to I_{Eqv}.

Single-cell upregulation

In a single cell, upregulation of TRPM4 channel expression lead to EADs at relatively modest increases (Fig. 4). This is not surprising given the large reduction in APD when it was removed. For increases above 2.12-fold nominal, the cells are no longer stable, and repolarization failure renders the cell unsuitable for propagation. In a mouse model of hypoxia and reoxygenation, pharmacological block of TRPM4 channel by 3-phenanthrol led to abolishment of EADs (18), indicating an important role of TRPM4 channels in EAD generation. For the slower PCL = 1000 ms, EADs occurred with each beat. At short cycle lengths, EADs only occurred after rapid pacing stopped. However, during pacing, the membrane voltage was rising just before the pacing beats were applied. It was quite different from resting potential.

Cable behavior

Central inhomogeneity

Activity in a 2-cm long cable was simulated using a finite element method with 100-μm linear finite elements. The central portion of the cable (see Fig. 5 *A*) had a different TRPM4 channel expression level than from the ends. The left end of the cable was paced with a transmembrane current stimulus at a PCL of either 600 or 1000 ms for 25 s. APs were detected as excursions in transmembrane potential of at least 40-mV amplitude with an APD_{80} of at least 70 ms, and cable behavior was categorized by analyzing the last 22 s of activity according to Table 1.

For low levels of TRPM4 channel expression, the cable conducted every pacing pulse with an activation time of 30 ms. As TRPM4 channel expression was increased beyond doubling, single cells had repolarization abnormalities, but the cells in the cable were still functional because of the electronic effects of neighboring cells. First-degree block occurred when the TRPM4 channel expression was increased in the midsection, leading to a very slow propagation to the right end. Second-degree block (see Fig. 6) was seen as TRPM4 channel expression continued to be increased in the midsection. In these cases, APs were not always present in the midsection, although a low voltage appeared to passively propagate across the midsection, which was sufficient to trigger an AP in the right end. Third-degree block was seen only at the slower pacing rate. At both pacing rates, the system became quiescent with high TRPM4 channel expression. The resting levels depolarized to such

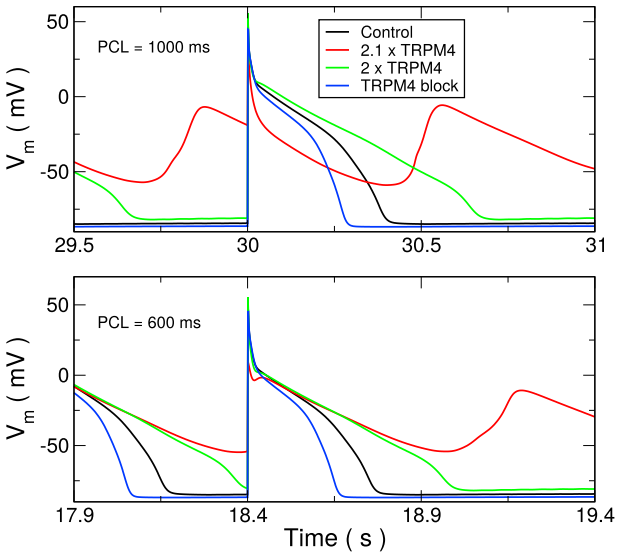

FIGURE 4 Single-cell AP traces for varying levels of TRPM4 channel expression. Colors indicate TRPM4 channel expression. Blocking the channel leads to significant APD reduction (*blue*) compared with control (*black*). A 2.0-fold increase (*green*) considerably prolongs APD, whereas a 2.1-fold increase (*red*) or more leads to early afterdepolarizations (EADs). Traces show last stimulated beats in a train of 30 at the indicated PCL. To see this figure in color, go online.

a high level that Na^+ channels could not regain excitability. With high TRPM4 channel expression levels in only one region (the ends or middle), pacemaking activity was also observed, more often at the slow pacing rate. Pacemaking activity was due to differences in resting potential level at the boundary between the high expression region and the low expression region. Because of electrotonic effects, the region of lower resting potential could be excited by the region of higher resting potential to generate spontaneous APs. For homogenous TRPM4 channel expressions (along the main diagonal), the cable conducts 1:1 and then becomes quiescent.

Linear gradient of TRPM4

We also implemented a linear gradient of TRPM4 channel expression in the same cable, stimulating again from the left end of the cable (Fig. 7). The left and right ends were independently assigned expression levels from 0 to 5 times control levels with a linear gradient in between for PCLs of 600 and 1000 ms. For a left level of control channel expression or less, there was always 1:1 propagation regardless of the right TRPM4 channel expression levels. For left expression levels at or above 3.5-fold control expression level, there was no propagation in the cable. For a left-end expression level in the range of 1.5 to 3-fold control, propagation only occurred when the right expression levels matched or exceeded the left-end levels. APs at the right end under these conditions were normal, and those on the left end showed rhythmic subthreshold activity at a frequency faster than pacing frequency.

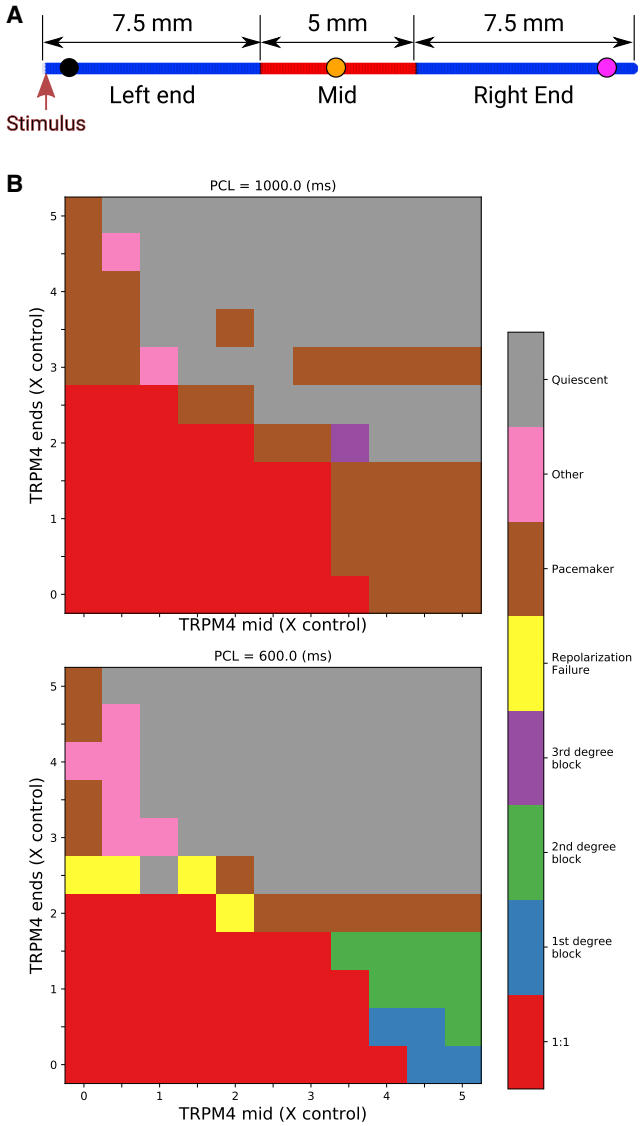

FIGURE 5 Cable simulations with central inhomogeneity. (*A*) Cable strand showing TRPM4 channel expression level regions. The left and right regions expressed same levels. Pacing stimuli were applied to the leftmost end of the cable. (*B*) Emergent behavior for different TRPM4 expression levels and PCL is indicated by color. See Table 1 for definitions. To see this figure in color, go online.

DISCUSSION

We have made several assumptions regarding the TRPM4 channel formulation, its reversal potential, and its constituent currents. We have shown its formulation cannot be simply added to existing models, so the channel must be already implicitly represented in the existing models. Based on channel current kinetics during AP, we decomposed it into background Na^+, transient outward K^+, and late Na^+ currents. We assumed that all of background Na^+ current in the original model was TRPM4 current and used this to calibrate the channel conductance. When we calculated the APD reduction in the final model with channel block,

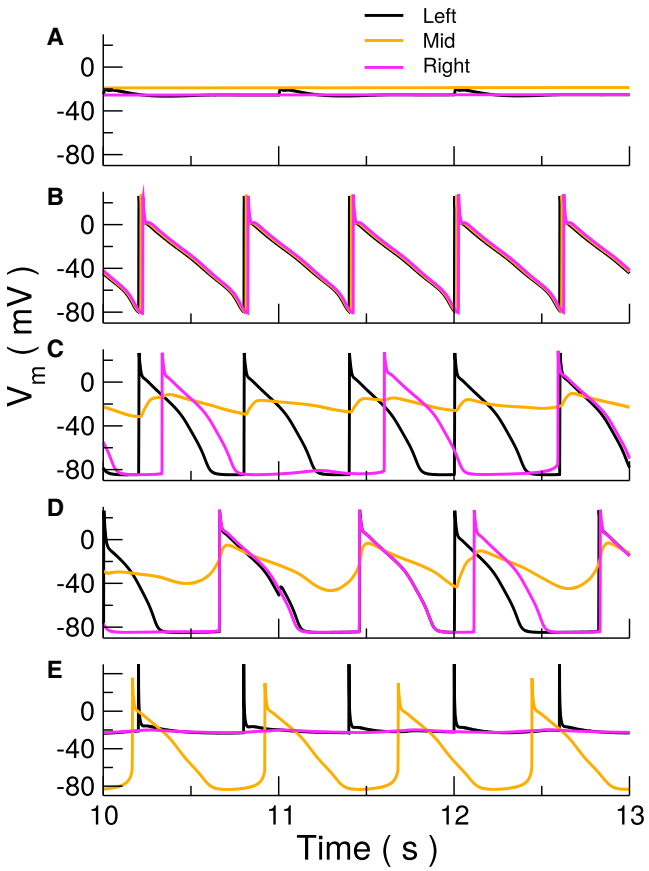

FIGURE 6 Simulated transmembrane voltage recordings from the left, middle, and right points of a Purkinje fiber. (*A*) Quiescence (4, 4, 600), (*B*) 1:1 (1, 1, 600), (*C*) type II block (1.5, 4, 600), (*D*) pacemaker from middle (1, 4, 1000), and (*E*) repolarization failure (4, 0.5, 600). Numbers in brackets indicate TRPM4 expression level at ends, in middle, and the pacing cycle length in ms, respectively. See Table 1 and Materials and Methods for definitions. To see this figure in color, go online.

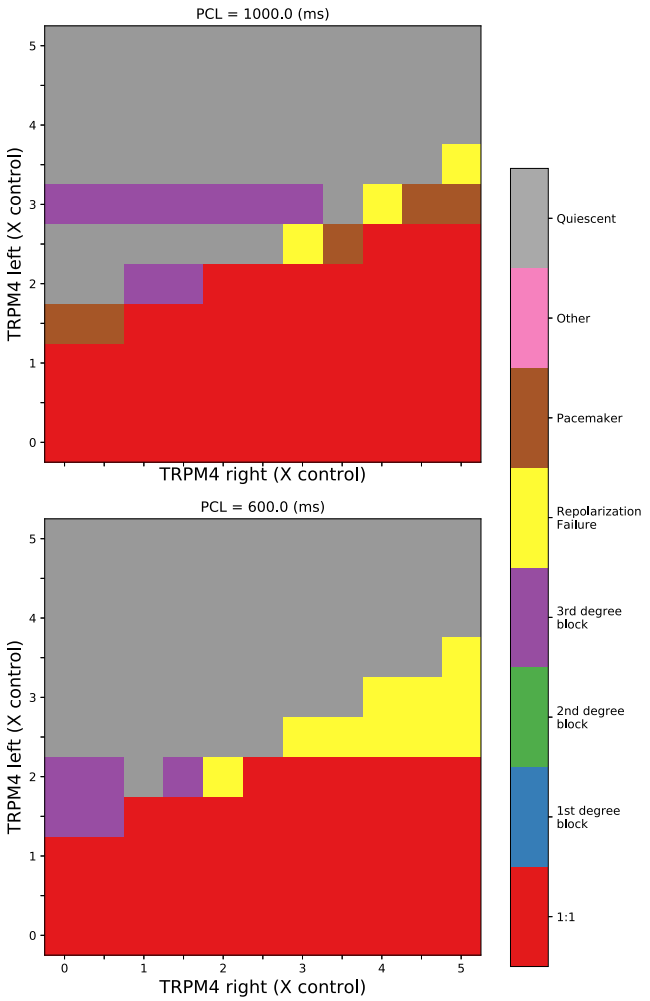

FIGURE 7 Cable simulations with a linear gradient of TRPM4 channel expression. Pacing stimuli were applied to the leftmost end of the cable, and the TRPM4 channel expression varied linearly in between. The emergent behavior for different TRPM4 channel expression levels and PCL are indicated by color. See Table 1 and Materials and Methods for definitions. To see this figure in color, go online.

it was close to that observed experimentally (13) (29.1 vs. 27%).

Based on the two spatial patterns of heterogeneity (linear and nonuniform TRPM4 expression along a cable) studied, it is found that a uniform high expression of TRPM4 channels will lead to quiescence. For propagation with a TRPM4 gain-of-function mutation, the region from which the pacing activity originates must have a lower expression level of TRPM4 than other regions. All degrees of heart blocks (type 1, 2, and 3) were seen in the simulations, depending on the TRPM4 expression levels, but nonuniform heterogeneity was requisite for any behavior beyond quiescence and 1:1 propagation. With a linear gradient, the behavior observed was limited, being 1:1 propagation if the levels were low enough, and for slightly higher levels, propagation if the gradient increased in the direction of propagation. First- and second-degree blocks were only seen with a nonuniform TRPM4 expression in the form of central heterogeneity. The central region could act passively to propagate the AP, leading to either a significant propagation delay or second-degree block. Interaction between two regions of different expression levels also led to pacemaking, although it was not always stable. The higher TRPM4 levels significantly depolarized the cells, which in turn excited the neighboring cells electrotonically. With the central heterogeneity, activity was more diverse at faster heart rates.

Families with TRPM4 overexpression have exhibited higher tendencies to present with heart block (5). Simulations here are consistent with these observations. We can generate third degree block depending on TRPM4 expression profiles. For first- and second-degree block, there has to be a heterogeneity in Purkinje cable properties. This can occur by differential expression of ion channels (e.g., TRPM4 channels) in different regions of PF network. The TRPM4 current has a very large effect on APD; it is the second-largest inward current during the plateau after I_{NaL2} and is the second-largest outward current during phase 1. Thus, global high

expression (i.e., greater than threefold control levels) would result in complete conduction failure of the His/Purkinje system. High expression levels have been estimated in patients with a TRPM4 mutation (5), but the spatial distribution was unknown. The propagation of electrical activity through the Purkinje system cannot be mapped, but small branches may be blocked in these patients. Given the complex and redundant network, these blocks may not always be detectable, but bundle branch blocks have been observed, and TRPM4 overexpression may explain it. For first- and second-degree blocks, the disruption would have to be quite proximal in the His bundle, otherwise impulses from the atrioventricular node (AVN) could still arrive early in the ventricles. Cheng et al. (19) concluded that I_{Nab} in the AVN of rabbits was not TRPM4 current. However, the full expression profile of TRPM4 channels across tissue and species has yet to be performed, so we do not know if TRPM4 channels are in human AVN. In other tissues, TRPM4 channels may also be responsible, at least in part, for I_{Nab} current, given its relatively large diastolic component. If human AVN is like rabbit AVN, this strengthens the argument that heart block observed clinically in patients with TRPM4 gain-of-function mutations, leading to its overexpression, are not due to AVN dysfunction because the channel is not present there but rather due to propagation impairment in the fast conduction system. Thus, it is more probable that the heart block observed arises from failure of the proximal His/PF to conduct.

Our TRPM4 channel current was mostly attributed to the background Na^+ current. Background currents exist in all ionic models for each ion and are the currents for which no specific protein has been identified. They are necessary to balance ionic fluxes over the course of the AP. A background current may represent a portion of a nonselective cationic channel current or several other currents that are not explicitly modeled. For example, the electrogenic glucose-Na^+ cotransporter-2 is usually not considered in electrophysiological models. Background currents are among the largest currents in cell models, as shown here, so if a new current is to be added to an existing ionic model, the background current must be adjusted, or the behavior of the model will deviate markedly from what was intended. We also demonstrated that adjusting a background current may not be sufficient, especially for nonselective channels. Because TRPM4 channels are significantly permeable to K^+ as well, a portion of an existing K^+ current had to be removed. In this case, it was observed that the transient outward K^+ current I_{to1} fit the same kinetic profile. There are many more TRPM channels (20) that have been identified proteomically and characterized at the channel level. However, their functional consequences and correspondence with known currents in cardiac cells remain unelucidated. They may, indeed, underly background currents found in other ionic models.

Our assignment of I_{Nab} to TRPM4 channels is in contrast to Cheng et al. (19) who found that TRPM4 channel was not responsible for I_{Nab} in mouse and rabbit AVN. However, expression of TRPM4 channels may differ across species and tissue type.

Limitations

Our modeling study is based on PRd. Our result that I_{TRPM4} is implicitly a combination of I_{Eqv} comprising I_{Nab}, I_{to1}, and I_{NaL2} is specific to this model. In particular, it was observed that in PRd, there is only one outward K^+ current I_{to1} during the phase 1 of AP and only one inward Na^+ current during the plateau phase that can match the profile of experimentally based I_{TRPM4}. The conductance of I_{TRPM4} was determined by I_{Nab} during the resting phase. There may be more uncharacterized Na^+ currents that can account for I_{Nab}. Other models of Purkinje cells may have more than one outward K^+ currents or Na^+ currents that match I_{TRPM4}. In that case, a sensitivity analysis should be performed to determine the principal components of I_{TRPM4}. We have used a simple model of cable simulations of PF and TRPM4 overexpression. A more realistic model of PF network and a complex distribution of TRPM4 overexpression may lead to different patterns of conduction abnormalities. However, our conclusion that heterogeneity of TRPM4 channel expression is required for intermittent heart blocks should still be valid in this case.

CONCLUSIONS

In this work, we have developed a, to our knowledge, novel formulation of TRPM4 channel current using relevant experimental data. TRPM4 channel is activated by both voltage and $[Ca]_i$ and can contribute significantly to the Purkinje cell AP. We incorporated this channel into the PRd model of Purkinje cell by subtracting an equivalent current composed of I_{Nab}, I_{NaL2}, and I_{to1} to match the dynamics of TRPM4 current during the AP. The model formulation matches experimental data. Rate dependence of APD, Na^+, K^+, and Ca^{2+} concentrations of the PRd model with TRPM4 is a close match to the original PRd model values. Upregulation of TRPM4 channel leads to EADs in a single cell. However, in cable only, a heterogenous distribution of TRPM4 channels led to intermittent heart block, type II, as seen clinically.

AUTHOR CONTRIBUTIONS

N.G. designed and performed research and wrote the manuscript. T.H. analyzed data and wrote the manuscript. M.H. designed the research. E.J.V. designed and performed the research, analyzed results, and wrote the manuscript.

ACKNOWLEDGMENTS

This study received financial support from the French Government as part of the Investments of the Future program managed by the National Research Agency (ANR), grant reference ANR-10-IAHU-04. This project has received funding from the Fondation Leducq (research grant number 16

CVD 02) and the European Research Council (Symphony, Grant Agreement N° ERC-2012-AdG_20120314).

REFERENCES

1. Launay, P., A. Fleig, …, J. P. Kinet. 2002. TRPM4 is a Ca2+-activated nonselective cation channel mediating cell membrane depolarization. *Cell.* 109:397–407.
2. Nilius, B., J. Prenen, …, T. Voets. 2005. The selectivity filter of the cation channel TRPM4. *J. Biol. Chem.* 280:22899–22906.
3. Guinamard, R., P. Bouvagnet, …, L. Sallé. 2015. TRPM4 in cardiac electrical activity. *Cardiovasc. Res.* 108:21–30.
4. Trafford, A. W., M. E. Díaz, …, D. A. Eisner. 1995. Comparison of subsarcolemmal and bulk calcium concentration during spontaneous calcium release in rat ventricular myocytes. *J. Physiol.* 488:577–586.
5. Kruse, M., and O. Pongs. 2014. TRPM4 channels in the cardiovascular system. *Curr. Opin. Pharmacol.* 15:68–73.
6. Kruse, M., E. Schulze-Bahr, …, O. Pongs. 2009. Impaired endocytosis of the ion channel TRPM4 is associated with human progressive familial heart block type I. *J. Clin. Invest.* 119:2737–2744.
7. Liu, H., L. El Zein, …, P. Bouvagnet. 2010. Gain-of-function mutations in TRPM4 cause autosomal dominant isolated cardiac conduction disease. *Circ Cardiovasc Genet.* 3:374–385.
8. Saito, Y., K. Nakamura, …, H. Ito. 2018. *TRPM4* Mutation in patients with ventricular noncompaction and cardiac conduction disease. *Circ Genom Precis Med.* 11:e002103.
9. Syam, N., S. Chatel, …, H. Abriel. 2016. Variants of transient receptor potential melastatin member 4 in childhood atrioventricular block. *J. Am. Heart Assoc.* 5:e001625.
10. Xian, W., X. Hui, …, P. Lipp. 2018. Aberrant deactivation-induced gain of function in TRPM4 mutant is associated with human cardiac conduction block. *Cell Rep.* 24:724–731.
11. Stallmeyer, B., S. Zumhagen, …, E. Schulze-Bahr. 2012. Mutational spectrum in the Ca(2+)–activated cation channel gene TRPM4 in patients with cardiac conductance disturbances. *Hum. Mutat.* 33:109–117.
12. Li, P., and Y. Rudy. 2011. A model of canine purkinje cell electrophysiology and Ca(2+) cycling: rate dependence, triggered activity, and comparison to ventricular myocytes. *Circ. Res.* 109:71–79.
13. Hof, T., L. Sallé, …, R. Guinamard. 2016. TRPM4 non-selective cation channels influence action potentials in rabbit Purkinje fibres. *J. Physiol.* 594:295–306.
14. Nilius, B., J. Prenen, …, V. Flockerzi. 2003. Voltage dependence of the Ca2+-activated cation channel TRPM4. *J. Biol. Chem.* 278:30813–30820.
15. Nilius, B., F. Mahieu, …, T. Voets. 2006. The Ca2+-activated cation channel TRPM4 is regulated by phosphatidylinositol 4,5-biphosphate. *EMBO J.* 25:467–478.
16. Vigmond, E. J., M. Hughes, …, L. J. Leon. 2003. Computational tools for modeling electrical activity in cardiac tissue. *J. Electrocardiol.* 36 (*Suppl*):69–74.
17. Hu, Y., Y. Duan, …, R. Inoue. 2017. Uncovering the arrhythmogenic potential of TRPM4 activation in atrial-derived HL-1 cells using novel recording and numerical approaches. *Cardiovasc. Res.* 113:1243–1255.
18. Simard, C., L. Sallé, …, R. Guinamard. 2012. Transient receptor potential melastatin 4 inhibitor 9-phenanthrol abolishes arrhythmias induced by hypoxia and re-oxygenation in mouse ventricle. *Br. J. Pharmacol.* 165:2354–2364.
19. Cheng, H., J. Li, …, J. C. Hancox. 2016. Characterization and influence of cardiac background sodium current in the atrioventricular node. *J. Mol. Cell. Cardiol.* 97:114–124.
20. Yue, Z., J. Xie, …, L. Yue. 2015. Role of TRP channels in the cardiovascular system. *Am. J. Physiol. Heart Circ. Physiol.* 308:H157–H182.